Proceedings of the 11th International Coral Reef Symposium, Ft. Lauderdale, Florida, 7-11 July 2008
Session number 17

Comparing Semi-Automated Methods for Classifying Multibeam SoNAR & Airborne LiDAR Imagery

B. Costa[1] and T. Battista[1]

1) NOAA Biogeography Branch, 1305 East West Highway, N-SCI-1 SSMC 4, Silver Spring, MD 20910, U.S.A.

Abstract. Benthic habitat mapping supports ecosystem-based management objectives by contributing to the development of detailed species utilization models, which link physical habitats to biological information. Shallow to deep-water marine habitats have been successfully characterized by manually digitizing and attributing optical and acoustic remotely sensed imagery. These resulting maps, while extremely useful, are subjective and ultimately irreproducible because they depend on the accuracy and interpretation of the person that is digitizing. Here, we semi-automate the seafloor feature extraction and classification process of high-resolution multibeam (MBES) sound navigation and ranging (SoNAR) and light detection and ranging (LiDAR) imagery using three classification techniques—Support Vector Machines (SVM), Classification & Regression Trees (DTC) and Object-based Segmentation (OBS). The ability and accuracy of these three techniques to delineate and characterize seafloor features was qualitatively compared at relevant spatial and thematic scales using georeferenced underwater imagery. Overall, we found that DTC and OBS out-performed SVM, as these two methods produced habitat maps that were qualitatively more accurate. This analysis suggests that DTC and OBS have the potential to help scientists more quickly and objectively characterize the seafloor, allowing resource managers to better assess the changing health of coral reef ecosystems.

Key words: LiDAR, multibeam SoNAR, MBES, coral reef ecosystems, benthic habitat mapping

Introduction

Benthic habitat mapping supports ecosystem-based management objectives by contributing to the development of detailed species utilization models, which link physical habitats to biological information (Friedlander and Parrish 1998; Pittman et al. 2007). Shallow to deep-water marine habitats have been successfully characterized by manually digitizing and attributing optical and acoustic remotely sensed imagery (Kendall et al. 2005; Battista et al. 2006). These resulting maps, while extremely useful, are subjective and ultimately irreproducible because they depend on the accuracy and interpretation of the person that is digitizing.

In the following study, we address this problem of subjectivity by semi-automating the seafloor feature extraction and classification process of high-resolution MBES and LiDAR imagery using three separate classification techniques. These three techniques—SVM, DTC and OBS—are fundamentally different in how they partition an image into separate classes.

SVM separates an image into classes by maximizing the margin between two groups of pixels in *n*-dimensional space (Vapnik et al. 1997). This margin is delineated using two parallel hyperplanes. The points nearest to these hyperplanes are called support vectors.

DTC separates an image into classes using binary recursive partitioning (Breiman et al. 1984), which is an iterative process whereby image pixels are split into two groups that are as homogenous as possible. The process continues until no more useful splits are found.

OBS separates an image into classes using edge detection algorithms (Haralick 1979; Blaschke et al. 2000). These algorithms detect the boundaries of homogenous groups of pixels. The pixels within each group are similar to each other based on a combination of characteristics, such as intensity and texture.

Given the methodological differences, we qualitatively compared these techniques to determine which was the most accurate, efficient and robust method for semi-automating the feature extraction and classification process. In doing so, we addressed the following key research questions:

(1) Which of these classification techniques most accurately delineated biologically & geomorphologically relevant habitats in Abrir La Sierra Conservation District?

(2) What are the strengths and weaknesses associated with each semi-automated classification technique?

Materials and Methods

Description of Study Site

The study site, Abrir La Sierra Conservation District, is a marine protected area (MPA) that is located 20 km off the western coast of Puerto Rico. This 16.7 km^2 region was designated as an MPA in 1996 due to concerns over declining reef fish populations (Waddell and Clark eds. 2008). The economically important species, red hind (*Epinephelus guttatus)*, was of particular concern because it uses Abrir La Sierra as a spawning aggregation site (SPAG). SPAGs are crucial to the ecology of an area because they help replenish fish populations, keeping their numbers relatively stable year after year. Since these aggregation sites are so vital, a concerted effort has been made to better understand them by mapping and monitoring changes in their associated benthic habitats.

Data Acquisition: System Specifications

Bathymetry and intensity imagery were acquired for the Abrir La Sierra using MBES and LiDAR. "Bathymetry" denotes the depth of the seafloor and was calculated by measuring the time required for an individual pulse of light or sound to travel from the sensor to the seafloor and back again. "Intensity" denotes the amount of light or sound that was scattered back to and recorded by the sensor. Data from both sensors were collected and processed to meet the International Hydrographic Organization Order 1 horizontal and vertical accuracy standards.

LiDAR data were acquired between 4/7 and 5/15/2006 for elevations between 19 m above sea level down to 50 m below sea level using a Laser Airborne Depth Sounder (LADS) Mk II Airborne System. This airborne system uses a 900 Hz neodymium-doped yttrium aluminum garnet laser, which is split by an optical coupler into an infrared (1064 nm) beam and a green (532 nm) beam. The infrared beam measures the datum height at nadir, and the green beam oscillates across-track to measure depths and/or elevations. The airborne survey was flown at altitudes between 1,200 and 2,200 ft. The raw data were logged using the Tenix LADS Airborne System and were converted using the LADS Mk II Ground System. The soundings were referenced to the NAD83 UTM 19 N horizontal coordinate system and to the Mean Lower Low Water (MLLW) vertical coordinate system (Stephenson and Sinclair 2006).

MBES data were acquired between 4/14 and 4/24/2007 for depths between 21 and 290 m using a Simrad 1002 (95 kHz) MBES. This hull-mounted, ship-board system has 111 electronically stabilized beams with 2° widths, rectilinearly arrayed 75° to the port and starboard of nadir. It achieves seafloor coverage of 7x water depth down to 1,000 m. The vessel's positioning and orientation were determined by the Applanix POS/MV 320 V4. The data parcels were logged using Kongsberg's MERLIN v5.2.2 acquisition and control program, and were referenced to the NAD83 UTM 19 N horizontal coordinate system and to the MLLW vertical coordinate system (Battista and Stecher 2007).

The LiDAR bathymetry and intensity surfaces were created at 4x4 and 5x5 m spatial resolutions (respectively) using CARIS Base Editor v2.0 software. The MBES bathymetry and intensity surfaces were processed and created at 5x5 and 1x1 m spatial resolutions (respectively) using CARIS Hips & SIPS v6.0 and Geocoder v3.2.1 software (Fonseca and Calder 2005). Both the LiDAR bathymetry and the MBES intensity surfaces were resampled to 5x5 m resolutions. All of the surfaces were exported as GeoTiffs and ingested into ArcGIS 9.2 for further analysis.

Ground Validation: Underwater Video Data
Georeferenced imagery of the seafloor was collected using NOAA Biogeography Branch's drop camera system between 4/14 and 4/24/2007. This system is equipped with lights, scaling lasers, an acoustic transponder, a digital video camera and a high resolution still camera (ccma.nos.noaa.gov/products/biogeography/usvi_nps/camera.html). The integration of these components allows for the collection of highly resolved and spatially accurate underwater imagery.

Each suitable, underwater image was visually interpreted and attributed by a trained observer using a hierarchical habitat classification scheme. This scheme defined broad and fine-scale benthic habitats on the basis of 13 geographic zones, 12 unique geomorphological structure types and 4 unique biological cover types using a variable minimum mapping unit (www8.nos.noaa.gov/bhv/bhvMapBrowser.aspx). The broad structure types included algal nodule pavement, bedrock, mud, pavement, sand and scattered coral and rock. The cover types included coral, macroalgae, turf and uncolonized. The resulting classified images were used to train the machine learning algorithms and to qualitatively validate the preliminary habitat classifications. A robust, quantitative accuracy assessment was not conducted because there were insufficient numbers of independent points (> 25) per unique thematic habitat class.

Data Processing: Surface Creation & Selection
A suite of metrics describing the complexity of the seafloor was created from the LiDAR and MBES bathymetric surfaces to aid in the identification and classification of benthic habitats. These morphometrics included: standard deviation of water depth, rugosity, slope, curvature & fractal dimensions (Table 1).

Each of these metrics were re-calculated at a range of spatial scales (10, 30, 50 & 75 m radii) using a median, circular moving window in ArcGIS 9.2. This multi-resolution approach was taken because fish and corals respond to benthic habitats at varying spatial scales (Kendal et al. 2003; Pittman et al. in press). These different metrics were then stacked in ENVI 4.4, creating a single composite image

Morphometric	Unit	Description	Analytical Tool
Standard deviation (SD) of water depth	Meters	Dispersion of water depth values about the mean	Focal statistic in ArcGIS Spatial Analyst
Rugosity	Ratio value	Ratio of surface area to planar area	Benthic Terrain Mapper toolbox (Jenness, 2002)
Slope	Degrees	Maximum rate of change in slope between cell and eight neighbors	ArcGIS Spatial Analyst's slope function
Curvature	1/100 z units	Rate of change in curvature across the surface highlighting ridges, crests and valleys	Curvature function in ArcGIS 3D Analyst
Fractal dimension (*D*)	Unitless	A measure of surface roughness with values between 2 and 3	FocalD script in LandSerf 2.2 (Wood, 2005)

Table 1. Description of morphometrics used to characterize and classify the homogenous habitats on the seafloor.

for each data type at each spatial scale (Fig. 1). The principal components of these composite images were calculated to determine the degree of correlation between pairs of metrics. The least correlated metrics were then included in the semi-automated classification.

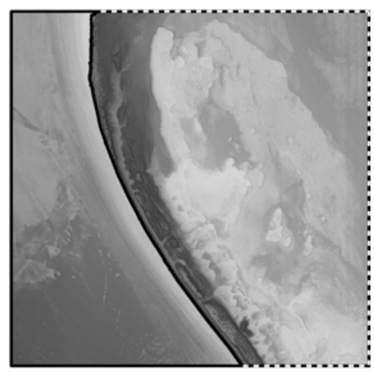

Figure 1. These composite images depict intensity, depth and slope surfaces as individual RGB bands. The imagery outlined by the black line (left) was acquired using MBES. The imagery outlined by the dashed line (right) was acquired using LiDAR.

Comparing Classification Methods
Several steps were needed to classify these composite images. The first step was to create regions of interest (ROIs) using the classified, video imagery. These ROIs were used to train each of the machine learning algorithms, which were subsequently deployed in ENVI original and ENVI Zoom v4.4. After each algorithm was run initially, the resulting outputs were refined by incrementally adjusting key input parameters. It was, however, difficult to objectively determine if these parameters were

optimized without being able to conduct a quantitative accuracy assessment. Such an assessment should be conducted in the future, allowing for the explicit optimization of these parameters.

The final step in this process was to visually compare the outputs from the three different methods to determine their qualitative accuracy. Surfaces with "high" qualitative accuracy: (1) did not confuse one habitat type with another; (2) did not identify geometric or radiometric artifacts in imagery as habitat features; (3) were capable of detecting subtle spectral differences between habitat types in the imagery; and (4) were capable of concurrently delineating fine and coarse-scale habitat features (e.g., individual patch reefs and aggregate patch reefs). Surfaces with lower qualitative accuracy did not meet one or all of these criteria.

Results

Classification Accuracy of LiDAR Imagery

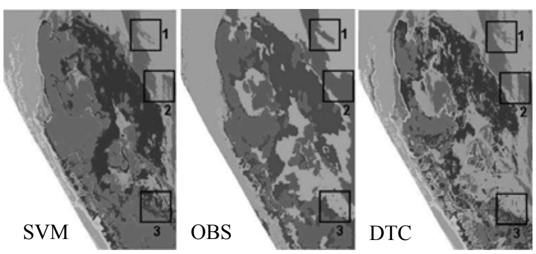

Figure 2. The final classified surfaces developed from the LiDAR imagery using SVM (left), OBS (middle) and DTC (right). Areas 1, 2 and 3 denote locations where the classified results did not meet one or several of the qualitative accuracy criteria as outlined above.

The three different machine learning techniques produced noticeably different classification results when applied to the LiDAR imagery. Overall, DTC produced (qualitatively) the most accurate result of the three methods. SVM and OBS produced less accurate results for two primary reasons: (1) they consistently confused one habitat class (sand) with another habitat class (low rugosity pavement) (Fig. 2, Area 1); and (2) they did not identify and extract many fine-scale features (reef holes) in the imagery (Fig. 2, Area 3). Despite DTC having produced a more accurate result, OBS was more resilient to geometric or radiometric artifacts in the imagery, and was less likely to identify them as habitat features (Fig. 2, Area 2).

Classification Accuracy of MBES Imagery

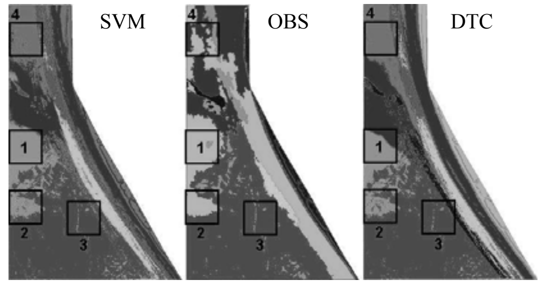

Figure 3. The final classified surfaces developed from the MBES imagery using SVM (left), OBS (middle) and DTC (right). Areas 1, 2, 3 and 4 denote locations where the classified results did not meet one or several of the qualitative accuracy criteria as outlined above.

The three different machine learning techniques also produced noticeably different classification results when applied to the MBES imagery. Overall, OBS produced qualitatively the most accurate result out of the three methods. SVM and DTC produced less accurate results for three primary reasons: (1) they consistently confused one habitat class (i.e., pavement) with another habitat class (i.e., bedrock) (Fig. 3, Area 1); (2) they consistently identified geometric or radiometric artifacts in the imagery as bona fide habitat features (Fig. 3, Area 2); and (3) they failed to detect subtle spectral differences between habitat types in the imagery (Fig. 3, Area 4). All three methods adequately extracted both fine and coarse-scale features simultaneously (Fig. 3, Area 3).

Discussion

A qualitative analysis of the three semi-automated techniques and their final, classified outputs revealed that each technique had specific strengths and weaknesses. These strengths and weaknesses were most likely the combined result of the algorithm's input parameters, the different spatial resolutions of the MBES and LiDAR surfaces, the shape of the re-scaling kernel, and the correlation between surface metrics. Changes to any of these parameters could have altered the classification results.

That being said, overall, DTC outperformed the other methods when applied to imagery with spectrally distinct habitats, and to imagery with few geometric or radiometric artifacts. It was also the fastest of the three methods, as it took the least amount of time to produce an accurate, classified image. OBS, on the other hand, was the slowest of the three techniques, albeit it did outperform the other methods when applied to imagery that had geometric or radiometric artifacts and to imagery that had habitats with similar spectral signatures. Overall, DTC and OBS both outperformed SVM because their surfaces had higher qualitative accuracies. SVM was most likely outperformed because it had many more parameters to adjust and optimize than did the two other methods.

A final benthic habitat map was created using the DTC surface developed from the LiDAR imagery and the OBS surface developed from the MBES imagery (Fig. 4). This seamless map characterized 18 unique seafloor habitats in 10 to 290 m of water.

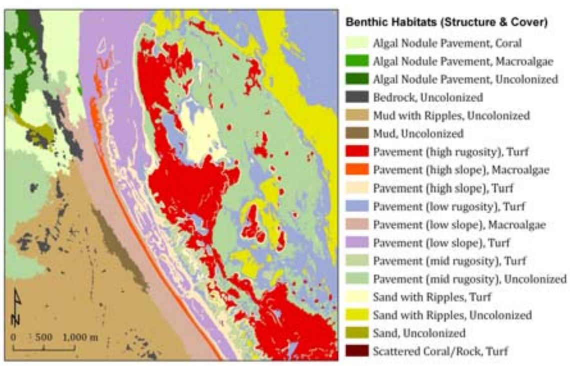

Figure 4. This graphic depicts the final, seamless benthic habitat map of Abrir La Sierra Conservation District. It was created by merging and edge matching the best classification outputs developed from the LiDAR and MBES imagery.

In conclusion, our current data and analysis indicate that DTC and OBS have the potential to help scientists create benthic habitat maps more quickly and efficiently. Future analysis (and a quantitative accuracy assessment) will improve this process further by objectively determining the optimal algorithm parameters. Hybridizing the OBS and DTC methods may also contribute to this improvement by integrating of the strengths of both techniques. The accuracy, objectivity and repeatability of habitat mapping will allow resource managers to more frequently and reliably assess the changing distribution (and ultimately, health) of the coral reef systems that they manage. Improving our understanding of these ecosystems is the key to identifying and mitigating the heterogeneous threats that face these important and precious resources.

Acknowledgements

The authors would like to thank Charlie Menza for processing and classifying the underwater photography. Also, special thanks to NOAA's Coral Reef Conservation Program for their continued support of the Biogeography Branch's effort to characterize coral reef ecosystems in the U.S. Caribbean.

References

Battista TA, Costa BM, Anderson SM (2007) Shallow-Water Benthic Habitats of the Main Eight Hawaiian Islands. NOAA Technical Memorandum NOS NCCOS 61, p 331.

Battista TA, Stecher M (2007) NOAA Data Acquisition & Processing Report: Project NF-07-06-USVI-HAB, p 111

Blaschke T, Lang S, Lorup E, Strobl J, Zeil P (2000) Object oriented image processing in an integrated GIS/remote sensing environment and perspectives for environmental applications. In: Cremers, A., Greve, K. (Eds.), *Environmental Information for Planning, Politics and the Public, vol. II*. Marburg, Germany: Metropolis-Verlag. pp 555-570.

Breiman L, Friedman JH, Olshend RA, Stone CJ (1984) Classification and regression trees. Belmont, California: Wadsworth International Group. p 324.

Fonseca L Calder B (2005) Geocoder: An Efficient Backscatter Map Constructor. Center for Coastal and Ocean Mapping, University of New Hampshire, p 9.

Fridlander AM, Parrish J. (1998) Habitat characteristics affecting fish assemblages on a Hawaiian Coral Reef. J Exp Mar Biol & Ecol 224:1-30.

Haralick RM (1979) Statistical and Structure Approaches to Texture. Proceedings of the IEEE 67:786-809.

Jenness J (2002). ArcView 3.x extension: Surface Areas and Ratios from Elevation Grid v1.2. Software extension freely available from: http://www.jennessent.com/arcview/grid tools.htm.

Kendall MS, Christenson JD, Hillis-Starr Z (2003) Muli-scale data used to analyze the spatial distribution of French grunts, *Haemulon flavolineatum*, relative to hard and soft bottom in a benthic landscape. Env Bio of Fish 66:19-26.

Kendall MS, Jensen OP, Alexander C, Field D, McFall, Bohne R, Monaco ME (2005) Benthic Mapping Using Sonar, Video Transects & Innovative Approach to Accuracy Assessment: A Characterization of Bottom Features in Georgia Bight. J Coas Res 21:1154-1165.

Pittman SJ, Christenson J, Caldow C, Menza C, Monaco M (2007) Predictive mapping of fish species richness across shallow-water seascapes in the Caribbean. Ecol Mod 204:9-21.

Pittman SJ, Costa B, Battista TA (in press) Using LiDAR bathymetry and boosted regression trees to predict the diversity and abundance of fish and corals. J Coas Res: Special Issue of Coastal Applications of Airborne LiDAR Remote Sensing.

Stephenson D, Sinclair M (2006) NOAA Data Acquisition & Processing Report. Project OPR-I305-KRL-06, p 49.

Vapnik V, Golowich S Smola A (1997) Support vector method for function approximation, regression estimation, and signal processing. In: Advances in Neural Information Processing Systems 9. Cambridge, MA: MIT Press. pp 281-287.

Waddell JE, Clarke AM (eds.) (2008) The State of Coral Reef Ecosystems of the United States and Pacific Freely Associated States. NOAA Technical Memorandum NOS NCCOS 73, p 569.

Wood J (2005) Landserf v2.2 software add-on: Focal-Dimension Calculation. Calculates a surface of fractal dimension values in a window around each raster cell. Software add-on freely available from: www.landserf.org.